ACS APPLIED MATERIALS & INTERFACES

Research Article

Highly Conductive and Flexible Nylon-6 Nonwoven Fiber Mats Formed using Tungsten Atomic Layer Deposition

Berç Kalanyan, Christopher J. Oldham, William J. Sweet, III, and Gregory N. Parsons*

Department of Chemical and Biomolecular Engineering, North Carolina State University, Raleigh, North Carolina 27695, United States

ABSTRACT: Low-temperature vapor-phase tungsten atomic layer deposition (ALD) using WF_6 and dilute silane (SiH_4, 2% in Ar) can yield highly conductive coatings on nylon-6 microfiber mats, producing flexible and supple nonwovens with conductivity of ~1000 S/cm. We find that an alumina nucleation layer, reactant exposure, and deposition temperature all influence the rate of W mass uptake on 3D fibers, and film growth rate is calibrated using high surface area anodic aluminum oxide. Transmission electron microscopy (TEM) reveals highly conformal tungsten coatings on nylon fibers with complex "winged" cross-section. Using reactant gas "hold" sequences during the ALD process, we conclude that reactant species can transport readily to reactive sites throughout the fiber mat, consistent with conformal uniform coverage observed by TEM. The conductivity of 1000 S/cm for the W-coated nylon is much larger than found in other conductive nonwovens. We also find that the nylon mats maintain 90% of their conductivity after being flexed around cylinders with radii as small as 0.3 cm. Metal ALD coatings on nonwovens make possible the solvent-free functionalization of textiles for electronic applications.

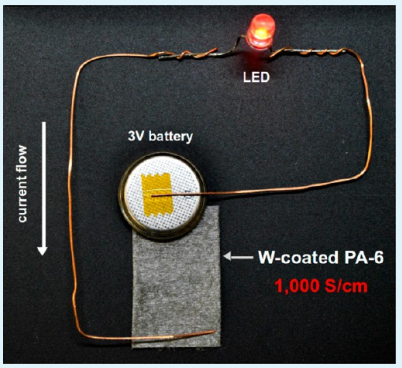

KEYWORDS: *tungsten, atomic layer deposition, conductive fibers, flexible electronics, nonwovens*

INTRODUCTION

Conductive fibers have applications in medicine, fluidics, catalysis, filtration, separation, energy storage, electromagnetic shielding,[1] smart textiles,[2] and chemical sensing.[2−4] Natural and synthetic fibers are made electrically conductive using a variety of methods including incorporation of metal fillers into fibers,[5] application of exterior conductive polymer coatings by in-solution polymerization[6] or spray-coating,[7,8] and core−shell fiber structures with conductive core or shell.[9] Fibers that incorporate organic conductive coatings or blends,[6,10−12] result in fibers with conductivity values less than 2 S/cm. Composite nanofibers containing oriented multiwalled carbon nanotubes reach about 1 S/cm conductivity[13] and Kevlar fibers coated with single-walled nanotubes result in 65 S/cm.[7] Metallic coatings on fibers have also been studied. Successively Ni- and Au-plated Kevlar fibers can display electrical conductivity values of 6 S/cm.[14] Silicone fibers filled with Ag flakes[5] reach 470 S/cm, whereas nylon fiber mats coated with Ag using a commercial electroless plating solution exceed ~1800 S/cm when loaded with ~17 wt % Ag.[4]

Another method of imparting conductivity to materials with complex geometries, such as nonwoven fabrics, is by applying coatings using vapor deposition techniques. In a previous work, we showed the application of tungsten coatings on woven quartz fiber mats by atomic layer deposition(ALD) for chemical sensing applications.[4] Here, we use the tungsten ALD process to coat nonwoven polyamide nylon-6 mats that have complex fibril cross sections. The atomic layer deposition process allows for precise thickness control and film conformality on complex and high surface area substrates. Furthermore, WF_6 and TMA employed in this study are common ALD precursors in the electronics industry. ALD processing is highly scalable and is more recently available in roll-to-roll configurations (e.g., Beneq WCS 500).

Tungsten ALD was first developed by adapting existing tungsten chemical vapor deposition (CVD) reactions.[15] Specifically, ALD of tungsten was conceived as a conformal nucleation layer for tungsten plug contacts typically prepared by CVD[16,17] for microelectronics applications. More recently, W ALD films were deposited on polymeric substrates,[18,19] nanoparticles,[20] and carbon nanotubes.[21] In this work, we expose nylon-6 mats to sequential doses of tungsten hexafluoride (WF_6) and 2% silane (SiH_4) diluted in argon in a flow-tube reactor to deposit tungsten thin films. We characterize the resultant conductive fibers using transmission electron microscopy, mass gain analysis, and four-probe conductivity. The W-coated fibers show excellent electrical conductivity and film conformality. Using the W-ALD process we reach conductivity values of 1000 S/cm which exceed most fabricated conductive fiber systems. The dry ALD process avoids common issues with substrate wetting and coating uniformity. We also show that W-coated nylon fiber mats maintain high conductivity upon bending around small cylinders. These features make W-ALD coated fibers attractive for flexible textile-based electronics or other related applications.

Received: March 26, 2013
Accepted: May 14, 2013
Published: May 31, 2013

   dx.doi.org/10.1021/am401095r | *ACS Appl. Mater. Interfaces* 2013, 5, 5253−5259

EXPERIMENTAL SECTION

We deposited tungsten in a custom built hot-walled ALD reactor housed inside a walk-in fume hood. The main reactor chamber consists of a 24 inch long stainless-steel tube with inside diameter of ~1.6 inches. Precursors are delivered into the reaction zone through 1/4-inch stainless steel tubes, heated to 70°C to preheat the process gas and prevent any precursor condensation. Pressure is monitored using a convection enhanced Pirani gauge installed downstream from the reaction zone, near the gas flow outlet. All gas flow rates are metered using needle valves and switched on and off by pneumatically actuated diaphragm valves. The reactor chamber was pumped by a rotary vane pump.

For aluminum oxide deposition we used 98% trimethyl aluminum (TMA) (Strem Chemicals) and reagent grade water (Ricca Chemicals) as precursors. The tungsten source was 99.9% tungsten hexafluoride (WF_6) from Sigma-Aldrich. The tungsten co-reactant was a dilute mixture (2% by weight) of silane in 99.999% Ar (Custom Gas Solutions, Durham NC). We used 99.999% pure N_2 as the carrier gas passed through an Entegris GateKeeper inert gas purifier to remove any residual water and oxygen from the nitrogen gas supply. Excess precursor and product gases are pumped out of the reactor using an Alcatel Pascal 2010SD (9.7 L/min) rotary vane pump filled with fluorocarbon oil (Fomblin 25/6 grade). Before reaching the pump, gases are scrubbed using two in-line filters (Visi-Trap by Mass-Vac Inc.).

Nylon-6 (polyamide-6, PA-6) samples used were hydro-entangled winged fibers down from Allasso Industries Inc., Morrisville NC. Because nylon-6 melts at 215°C[22] we limit deposition to a maximum temperature of ~200°C. The fiber mat basis weight is 70 g/m^2, and the Brunauer Emmett Teller (BET) specific surface area was measured to be 2.5 m^2/g using a Quantachrome Autosorb-1. Anodic aluminum oxide (AAO) disk substrates were purchased from Whatman (Anopore Anodisc). The disks were 13 mm in diameter and 60 μm thick, and the average pore diameter was 200 nm. Silicon wafers for process monitoring were purchased from WRS Materials (wafers manufactured by MEMC) and were used as received.

Before each tungsten deposition, the carrier gas pressure was adjusted to 2.0 Torr. P-type silicon (100) wafers were cleaved into 1 × 1 cm pieces and loaded into the chamber using a flat sample boat, positioned at the midpoint of the reaction zone (12" downstream from gas inlet). The fiber and AAO substrates were held in place two pieces of fine stainless steel mesh. The silicon and fiber samples were placed in the reactor so that precursor gases flowed parallel to the samples (i.e. perpendicular to the sample normal), whereas the AAO samples were positioned upright in the reactor (gas flow parallel to the sample normal, i.e., "flow-through" configuration) to help promote gas transport through the substrates.

After loading the samples, the reactor was pumped down to 80 mTorr followed by dry N_2 flow for 30 minutes at the operating pressure between of 2.0 Torr to allow the sample to reach the reaction temperature. Prior to tungsten deposition, all samples were coated with 25 cycles of Al_2O_3 in order to promote W nucleation.[23,24] One ALD cycle for aluminum oxide consisted of the sequence TMA/N_2/H_2O/N_2 with times of 0.3/30/0.3/30 s respectively, producing 1.1–1.2 Å of growth per cycle. Film thickness was measured after deposition using spectroscopic ellipsometry (J.A. Woollam Co. alpha-SE) with the CompleteEASE data analysis software package. The Al_2O_3 optical constants were obtained by fitting ellipsometry data from a ~100 nm alumina film on silicon to a Cauchy model. The typical native silicon oxide thickness was measured to be ~1.7 nm and was included in the model.

Tungsten ALD films were deposited by dosing 2% SiH_4 and WF_6 precursor gases into the reactor in alternating pulses. The pulse sequence followed the $WF_6/N_2/SiH_4/N_2$ pattern with typical exposure times of 1/30/45/30 seconds. For some runs, we used a "hold" step where we closed all the valves in the reactor immediately after a precursor dose in order to expose the sample to precursor vapor for an extended period of time. We recently studied the effect of silane exposure and deposition temperature on W ALD using WF_6 and dilute silane.[25] Using silane and WF_6 exposures of ~6×10^5 and ~1×10^6 Langmuirs, respectively, we find an ALD "temperature window" between 200 and 300 °C with a W growth rate of ~6.0 ± 0.5 Å/cycle. At 150 °C, a silane exposure of 6×10^5 L leads to saturated growth at ~4 Å/cycle. Using 2% silane in Ar, this exposure is attained for a 30 s exposure when the pressure change during the SiH_4/Ar dose is controlled at 1.0 Torr.[25] In this work, we investigate the role of silane and WF_6 dose on mass uptake and effective conductivity of the coated nylon fiber mats.

The gas exposure is estimated by the net pressure change multiplied by the dose time. When the WF_6 cycle produces ΔP = 0.2 Torr, a 1 second gas pulse time corresponds to 0.2 Torr × 1 s = 2.0×10^5 L exposure. For the 2% silane in argon, the exposure times are longer, so for ΔP = 0.5 Torr, a 30 s gas pulse time corresponds to 0.5 Torr × 0.02 × 30 s =3.0×10^5 L. These exposure values are rough estimates. The analysis neglects gauge sensitivity to non-inert gases, the contributions of reaction by-products to the measured pressure, as well as effects of gas flow dynamics (including pressure transients and any composition-dependent pumping speed). We use these estimates only to compare relative exposures under various run conditions.

Growth rate on fibers was determined by measuring the mass of the substrate before and immediately after deposition (Fisher Scientific Accu 124 mass balance). The percent mass gain is the difference between the mass before and after coating divided by the starting mass. All of our nylon samples were cut into uniform sizes from the same fabric stock.

Conductivity of tungsten-coated nylon-6 fiber mats was measured using a four-probe apparatus.[4] Briefly, coated fiber substrates were contacted by four parallel gold contact pads with the outer electrode pair connected to a current source and the inner pair connected to a volt meter (Keithley 2400 source meter). Samples were then subjected to a normal compressive force of known magnitude to enhance contact between the individual fibers. Assuming that the conductive coating is uniform between the electrode contacts, the effective conductivity of the coating was determined by normalizing to the coating mass and coating material density (taken to be the coating material bulk density). For comparison, the resistivity of tungsten films on oxide-coated silicon was measured using a Jandel four-point probe with an RM3-AR head.

Transmission electron microscopy was performed on nylon-6 fiber samples prepared by microtome (Leica Ultracut 7 equipped with a diamond knife). The fibers were embedded in Spurr's epoxy (EMS) and cured using a standard curing schedule. The embedded fibers were cut at room temperature into 90–110 nm thick slices. Sections collected on 300 mesh sample holder were imaged using a cold field emission electron source with an accelerating voltage of 200 kV (Hitachi HF2000).

Porous AAO samples were imaged in an FEI XL30 scanning electron microscope system equipped with a field emission electron gun. Prior to imaging, bare AAO samples were coated with Au/Pd (80%/20%) for 2 min in a sputter coater. Tungsten ALD coated AAO samples did not require any sputtering due to the high conductivity of the thin films.

RESULTS AND DISCUSSION

W ALD Growth Rate Calibration on Anodic Aluminum Oxide. As a first step in characterizing tungsten deposition on nylon substrates, we deposited tungsten films on commercial anodic aluminum oxide substrates and examined film thickness by SEM and TEM. These substrates have an effective aspect ratio of >300:1, which is larger than that for the nonwoven nylon fibers mats. Although the effect of gas exposure and reactant 'hold' times were not explored for these structures, we used hold steps for TMA, H_2O, and WF_6 doses. The silane doses consisted of long exposure times (i.e. 120 s) without hold steps. After coating with 25 cycles of Al_2O_3, we deposited 25, 45, or 100 cycles of W, all at 200°C. The Al_2O_3 recipe was TMA/N_2/H_2O/N_2 = 0.3(20)/60/0.3(20)/90 s, respectively.

Similarly, the W ALD cycle followed $SiH_4/N_2/WF_6/N_2$ = 120/90/1(60)/60 s. The pressure change in the reactor was 1.0 Torr during the 2% silane dose and the WF_6 dose.

Figure 1 shows a series of plan-view SEM images of the partially filled AAO pores after Al_2O_3 and W ALD.

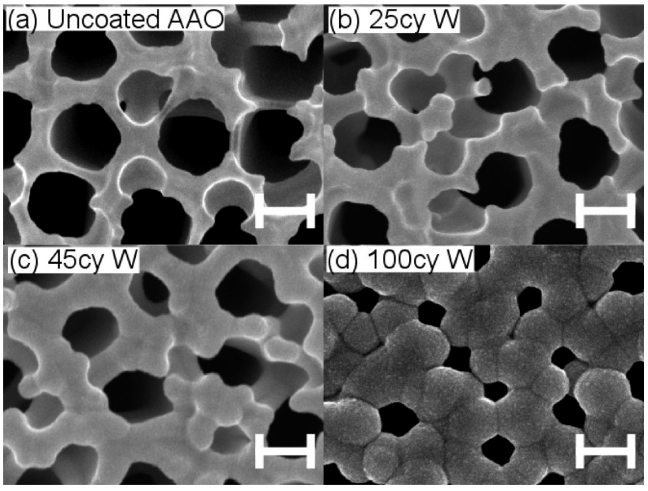

Figure 1. Top-down SEM micrographs of anodic aluminum oxide samples treated with different thicknesses of ALD tungsten at 250 000× magnification (scale bars are 200 nm). The imaged AAO substrates have approximately 250 nm diameter pores. (a) Uncoated substrate. (b–d) Images collected after 25 cycles of Al_2O_3 and 25, 45, and 100 cycles of W, respectively, at 200 °C. These images show pore shrinkage due to increasing ALD coating thicknesses. Samples coated with higher cycle numbers show increasingly rounded edges and softer features in the nanometer scale due to the conformality of the coatings.

Figure 1a shows an uncoated AAO substrate coated with a thin Pd/Au layer to facilitate electron imaging. The pores are not highly uniform, but the average diameter is estimated to be 251±14 nm. Image (b) was collected after 25 W ALD cycles. Average pore diameter is reduced to 212 ±13 nm after the ALD coating. Edge definition is also lost to some extent, as features appear less sharp. After 45 W cycles, image (c) shows pore sizes further reduced to 186 ± 30 nm and edge features are rounded as would be expected from a conformal coating. Increasing the coating thickness to 100 cycles in image (d), the average pore diameter becomes 94±17 nm. Some smaller pores appear to be closed completely and the top surface of the AAO is rounded. The change in pore size yields a growth rate of ∼7.8 Å/cycle. Considering the nonuniform starting surface, this is reasonably similar to the ∼6 Å/cycle we observed on planar Si(100) substrates coated separately under similar conditions.[25] Growth thickness versus cycle number for deposition on AAO (from TEM) and on silicon are shown in Figure 2.

We also verify the thickness of the W films in AAO by imaging the pores at an angle. Figure 3 shows micrographs of W-coated AAO after mechanical breaking.

In addition to a cross-section view of the W coating, the cracking also removed parts of the AAO walls to reveal the W formed along the inner pore walls (see for example the arrow in Figure 3a). The coating in image Figure 3b is ∼2× thicker than in (a), consistent with the increased coating cycles. The W growth rate from these images is 6.6 Å/cycle. The results on AAO confirm that the W ALD process using dilute silane can produce controllable W ALD coatings on high-aspect-ratio structures.

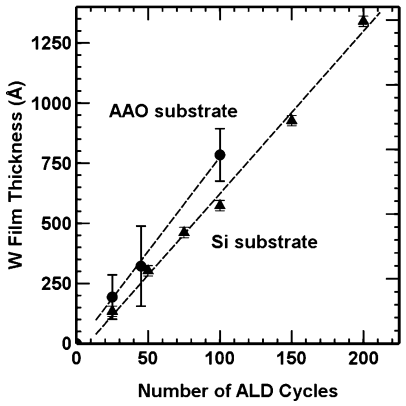

Figure 2. Tungsten film thickness versus ALD cycle number on AAO and silicon substrates. Samples are pretreated with 25 cycles of Al_2O_3 and processed at 200°C. Film thicknesses on the AAO were extracted from top-down SEM images of AAO pores shown in Figure 1.

W ALD Nucleation and Conformality on Nylon-6 Nonwovens. Although the amide functional group in nylon-6 is reactive with trimethylaluminum, and to a lesser extent, with diethyl zinc,[26,27] the reactions for direct deposition of W from WF_6 and SiH_4 on nylon are not known. Tungsten ALD on various polymers including polyethylene, polyvinyl chloride, polystyrene, polycarbonate, polypropylene, polymethylmethacrylate, Kapton polyimide and polyethylene naphthalate has previously been reported,[19,24] and results show that W ALD nucleates well when the polymer is pretreated with several cycles of ALD Al_2O_3. We find that a thin (25 cycle) Al_2O_3 pretreatment also helps promote W nucleation on nylon-6. Figure 4 shows a bare fiber next to nylon-6 fiber samples after 100 W ALD cycles at 140 °C, with and without 25 cycles of alumina pretreatment.

The sample without pretreatment shows no visible tungsten nucleation and is electrically resistive when measured with the four-probe apparatus. The pretreated sample shows a uniform tungsten coating and shows good overall conductivity (as discussed later on). Previous infrared analysis of TMA/H_2O on nylon fibers showed significant sub-surface precursor diffusion, reaction, and nucleation during ALD at 90°C, producing detectable nuclei more than 100 nm from the fiber surface.[26,28] The alumina pretreatment used here was done at the same temperature as the W ALD (between ∼140 and 200 °C), so alumina is expected to be present on and below the surface of the nylon fiber.

Transmission electron micrographs from PA-6 samples with 25 cycles of alumina pretreatment and 100 cycles of W are shown in Figure 5.

The cross-sectional images show the high surface area "winged" structure of the fiber. The dark contrast in the images corresponds to the tungsten coating which is uniform and conformal on the fiber. The highest magnification image (panel c) shows a "wing" edge where the apparent layer thickness is ∼75 nm. The actual film thickness is difficult to quantify for polymers after microtome sectioning. The microtome slice is in the range of ∼100 nm, so it is possible that when the microtome cuts the relatively soft polymer, the hard metal coating folds partly onto its side, distorting the thickness analysis. The metal film can be thought of as a ribbon or a strip wrapped conformally around the fiber. When a cross-section is cut by mechanical shearing, the metal strip may twist, exposing its planar side to the electron beam, rather than its line edge.

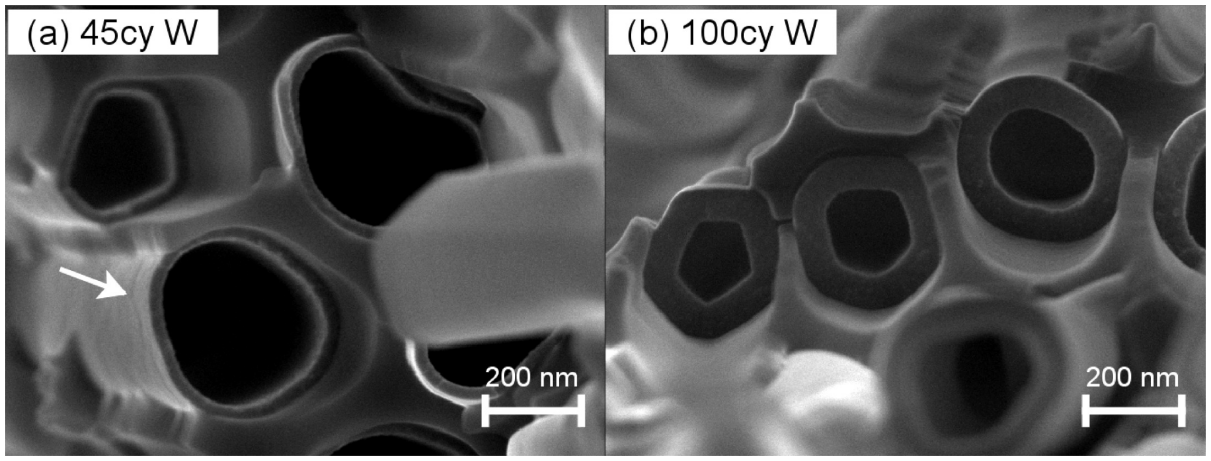

Figure 3. Cross-sectional view of AAO pores with: (a) 45 cycles; and (b) 100 cycles of W ALD after breaking the coated AAO. The AAO templates are pre-treated with 25 cycles of Al_2O_3 and processed at 200°C. In each image, an inner tube of tungsten is surrounded by an outer AAO substrate shell, and the W thickness increases with ALD cycle number. The arrow in image (a) points to the outer side-wall of a W tube where the AAO shell was removed.

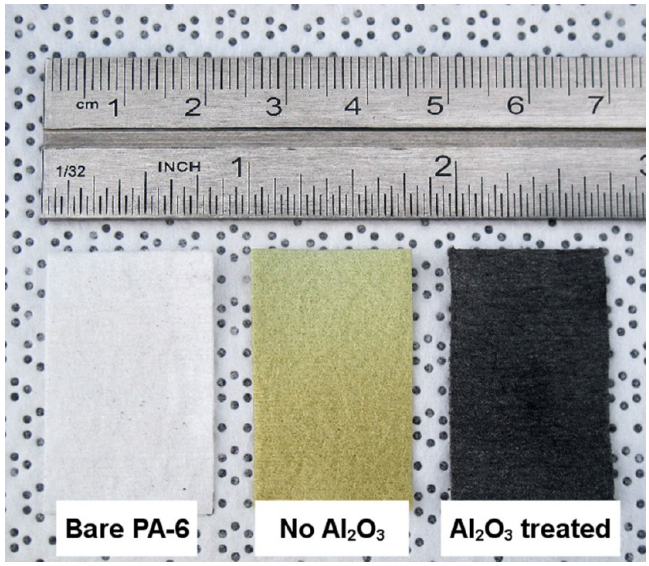

Figure 4. Photograph showing nonwoven nylon-6 fiber mats after coating with 100 cycles of W ALD at 140°C. The sample on the left is not treated with Al_2O_3, resulting in poor tungsten nucleation on the fibers, whereas the sample on the right shows proper W nucleation as a result of pre-treatment with 25 cycles of Al_2O_3 at 140°C.

What appears to be film thickness nonuniformities, especially visible in panels (a) and (c) on the wing tips, are likely an artifact of TEM sample preparation.

Effect of WF_6 and SiH_4 Exposure on W ALD on Nylon Fibers. We explored the effect of temperature on mass uptake for W ALD on nylon. Using silane and WF_6 exposures of ~4.5 × 10^5 and ~2 × 10^5 Langmuirs, we see minimal growth at T < 140°C, with more growth at higher temperatures up to 180 °C. The amount of W deposited during the WF_6 exposure half-cycle is affected by the amount of silicon left on the growth surface during the previous silane half-cycle step.[29] Tungsten ALD can be achieved at near room temperature using very large silane and WF_6 exposure steps. For example, Wilson et al.[24] report good W ALD at 80°C using repeated static Si_2H_6/WF_6 doses which produce large gas exposures. For some runs, we also observe anomalously low growth rates, especially at higher temperatures near 200°C. The decreased deposition on the polymer fiber is ascribed to reactor wall effects in our tubular hot-wall reactor system. Specifically, under the high silane exposures used here, the reaction between SiH_4 and the W surface is thermally activated, so silane may be consumed upstream on the walls before a sufficient amount reaches the high surface area fiber mat substrate. Studies of the dilute silane process[25] suggest that the silane depletion occurs even when the reactor walls are pretreated with a thin (2−3 nm) layer of alumina. Pretreating the reactor wall with large silane doses before loading the substrate (and before depositing the alumina nucleation layer) appears to eliminate the unexpected low growth rates.[25] Although the mechanisms are not clear, these observations suggest that the thin alumina nucleation layer may permit some transport of silicon species.

Tungsten and silane exposure affect W growth on the nylon mats. Mass uptake saturation as a function of silane and WF_6 exposure is shown in Figure 6 for deposition at 145°C.

For varying WF_6 exposures, the silane pulse was fixed at ~4.5 × 10^5 L, and for varying SiH_4 exposures, the WF_6 was fixed at ~2 × 10^5 L. The mass uptake increases with both SiH_4 and WF_6 exposure, although the rate is more sensitive to the silane exposure in the range studied. Using the sample basis weight, measured fiber surface area, and expected W density, the mass uptake values are ~2× smaller than expected for uniform ~3 Å/cycle at 145°C.[25] The BET surface area for the complex 3D network measured using N_2 adsorption may be larger than the surface area that can be reached by the SiH_4 and WF_6 precursors. Figure 7 shows the effective conductivity for the same samples in Figure 6 prepared with various SiH_4 and WF_6 exposures at 145°C, and we find that the conductivity is nearly constant at ~1000 S/cm when the precursor doses produce sufficient deposition.

Reactant Species Transport through the 3D Fiber Network. It is important to understand if the growth on the fibers is limited by reactant species transport through the fiber network. That is, we want to know if the ALD process sequence is sufficient for the reactants to fully reach all exposed surface area within the nonwoven fiber mat during the specified gas pulse times. The TEM images in Figure 5 show good conformal coverage over the areas examined, demonstrating complete exposure at the sites imaged. The mass change after ALD

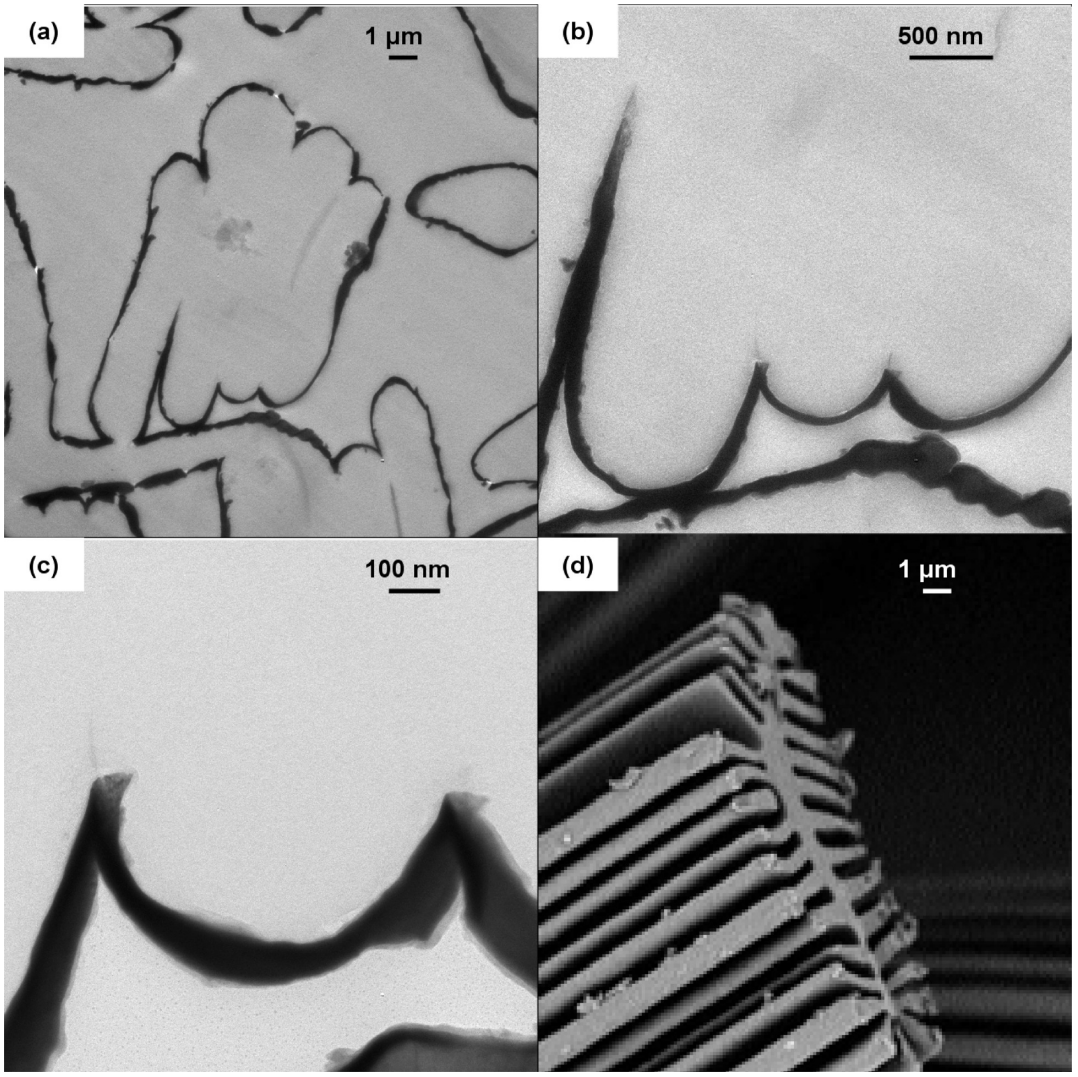

Figure 5. Micrographs of nylon-6 fibers (Allasso, Winged Fibers) coated with 25 cycles of Al_2O_3 followed by 100 cycles of W at 160 °C. The dark contrast is from the tungsten coating, which grows conformally around the fiber wings. The Al_2O_3 deposition is not visible at these magnifications. (d) Cross-sectional SEM image of a PA-6 fibril. Reproduced with permission from Allasso Industries Inc. Copyright Allasso Industries Inc.

coating, however, can give insight into the extent of reaction over the entire surface area of the fiber. Mass change analysis with W ALD works particularly well because of the high density of the W metal. Working specifically in the sub-saturation gas exposure region, i.e., where the extent of reaction is sensitive to the amount of reactants reaching the growth surface, we can use the mass change to explore the extent of reaction and thereby probe reactant transport effects. To probe reactant transport, we introduce a reactant "hold" step into the process sequence. Specifically, after a 10 s SiH_4 dose, we closed the reactor valves to cease the gas flow for some period of time (20−120 s) then opened the valves to purge for 30 s. The cycle then finished with the same 1 s WF_6 exposure and 30 s N_2 purge. The reaction sequence for a 10 s silane dose with a 60 s SiH_4 hold, for example, is denoted as $SiH_4/N_2/WF_6/N_2$ = 10(60)/30/1/30 seconds. This "hold" step provides time for gas that is in the chamber to diffuse and move through the tortuous fiber structure. This differs from a longer pulse time, where gas flow continues to supply reactant. If the growth is limited by the reactant transport through the fiber network structure, the hold steps will give reactants more time to reach reactive sites, leading to a net increase in film growth. If species transport is facile through the network, the reaction will go to completion during the pulse time and the hold time will not significantly affect the overall mass uptake.

For this analysis, we also consider the total fiber surface area. The fiber mat has a basis weight of 70 g/m^2 and the BET surface area is 2.5 m^2/g so the surface area per unit 2D area of fabric sample is ∼175 m^2/m^2. This surface area value can be roughly related to a trench aspect ratio, where 175 m^2/m^2 corresponds to a set of equally spaced vertical trenches with aspect ratio of ∼175:1. This aspect ratio is reasonable for conformal coating by ALD. However, unlike vertical trenches on a fabricated semiconductor wafer, the fiber mat surface includes many "hidden" regions with variable sizes and shapes, well outside the line-of-sight. This complex 3D structure will likely affect the growth, and the hold sequence may help improve uniformity.

We test effects of species transport through the fiber mat by comparing changes in mass when we change: (i) silane gas pulse time; or (ii) silane hold time with fixed silane pulse time. We started with silane pulse times less than the full saturation exposure where mass uptake will be sensitive to the number of reactant/surface interactions. Using the same conditions as

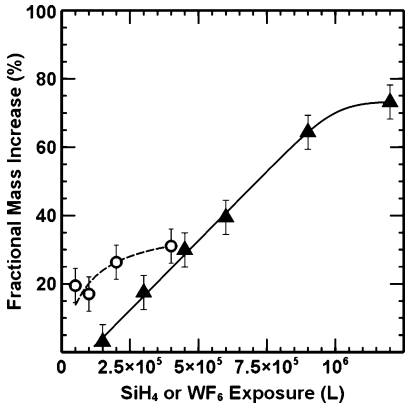

Figure 6. Effect of SiH_4 and WF_6 exposure on substrate mass gain after 25 Al_2O_3 cycles and 100 W ALD cycles at 145°C. The data points show mass uptake on the nylon fiber mat for: (closed triangles) increasing silane exposure with fixed WF_6 exposure ($\approx 2 \times 10^5$ L); and (open squares) increasing WF_6 with fixed silane exposure ($\approx 4.5 \times 10^5$ L). The pressure change during silane and WF_6 doses was 0.5 and 0.2 Torr, respectively. For films with 20% or more mass loading, the maximum error of the mean for fractional mass increase was ± 5%, as shown by the error bars. The lines are a guide for the eye.

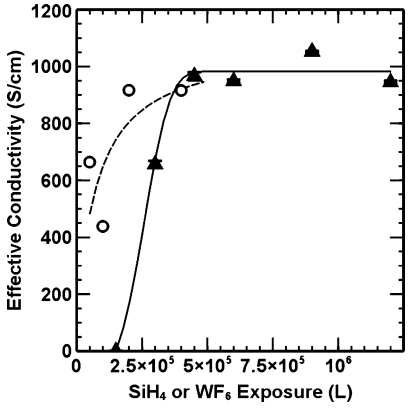

Figure 7. Fiber mat effective conductivity as a function of SiH_4 and WF_6 exposure for 25 cycles of Al_2O_3 and 100 cycles of W deposition at 145 °C. The data symbols correspond to the samples shown in Figure 6. The conductivity is approximately 1000 S/cm, independent of exposure conditions when sufficient coating thickness is present. The lines are a guide for the eye. Each data point represents an average of 7 measurements for each sample. The standard error of the mean is smaller than the size of the data points.

used for the data in Figure 6, we performed 100 ALD cycles at 145 °C with and without hold steps, and results are shown in Figure 8.

The data show that increasing the silane gas flow time from 15 to 120 s without the hold sequence leads to increased mass, whereas the silane hold step after a fixed 10 s silane flow does not increase mass uptake. This indicates that the relatively short gas dose time is sufficient for silane to reach reactive sites throughout the fiber matrix under the conditions investigated. Different growth conditions or different fiber size, density, or composition will affect reactant transport, so we sometimes use reaction hold steps to help ensure uniform surface reaction.

Mechanical Response of W-Coated Nylon-6 Nonwovens. We are also interested in the mechanical response of the W-coated nylon fiber samples. After coating, the microfiber mat still retains the "soft" feel of the uncoated fabric,

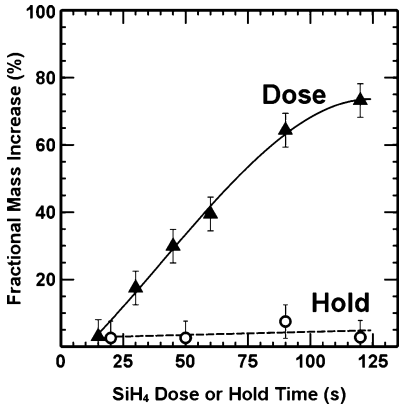

Figure 8. Effect of varying silane dose times and short silane doses combined with varying hold times on W mass uptake on nylon-6 fiber mats. All samples were coated with 25 Al_2O_3 and 100 W cycles at 145°C. For the "hold" sequence, the silane dose time is set at 10 s, after which the reactor is closed for a set hold time between 20 and 120 s. The remainder of the ALD cycle was unchanged. We also compare runs done with different silane dose times without the hold step (triangle symbols, data from Figure 6). With the 10 s silane exposure, the hold step does not enhance W mass uptake on the fiber mat substrates. The error bars represent an uncertainty of ±5% in the mass loading analysis.

suggesting that the W-coated fibers retain flexibility. To test the flexibility of the coated fibers, we measured conductivity after bending the fiber mats around radii of increasing curvature. We first measuring conductivity with the sample laid flat in our test apparatus then we molded the mat around a large cylinder. The sample was then laid flat again to measure conductivity. This was repeated several times for the same fiber sample bent around cylinders of decreasing radius, and the results are shown in Figure 9. This procedure is described more fully in ref 30.

Also shown are results from similar analysis[30] of a conductive ZnO layer conformally deposited by ALD onto a polypropylene fiber mat. The results show that the W-coated nylon retains

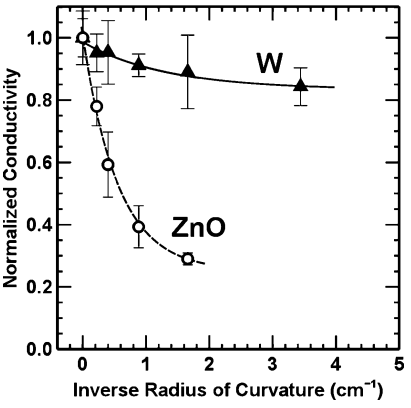

Figure 9. Change in conductivity for conducting layers deposited on fiber substrates when the fiber mats are bent around increasingly smaller cylinders. The conductivity of ZnO on polypropylene fibers is approximately 20 S/cm as prepared, but it decreases substantially upon bending. Similar experiments for the W-coated nylon studied here shows ~90% conductivity retention upon bending. Data from ZnO coated polypropylene is from ref 30. Tungsten-coated samples were prepared with 25 Al_2O_3 and 100 W cycles at 145°C. Each data point represents the mean of two conductivity values collected from each sample, and the error bars show typical variation.

~90% of its conductivity after bending around a radius as small as 3 mm, and the performance is much better than ZnO material. This suggests that W-coated nylon may be a good material for future flexible electronic systems integrated with textiles.

SUMMARY AND CONCLUSIONS

We successfully used WF_6 and 2% SiH_4 in Ar in an ALD sequence to produce conductive coatings on nylon-6 fiber mats at 145°C. Pretreating the fiber mats with 25 cycles of TMA/H_2O ALD helps promote W nucleation. The W mass uptake on the nylon fiber mats shows saturated behavior with increasing silane and WF_6 exposure. The process offers good thickness control and produces conformal coatings on fiber mats and on nanoporous and high aspect ratio alumina structures. High surface area winged nylon-6 samples coated with W ALD show very high effective conductivities in the 1000 S/cm range, and the conductivity remains high even after bending around a small diameter. Good conductivity can be achieved with less than ~20% mass loading. The conductivity values we measure greatly exceed those reported in previous studies using electrospinning, injection forming, and bulk treatment techniques.[31−33] Results demonstrate that the dilute SiH_4/WF_6 process is suitable for producing high-quality conductive nylon-6 nonwoven fiber mats, which may enable electronic structures to be integrated into nonwoven or textile media. Potential applications for conductive fiberous media include chemical sensing, wearable electronics, biomedical devices, and energy conversion and storage.

AUTHOR INFORMATION

Corresponding Author

*E-mail: bkalany@ncsu.edu.

Funding

We acknowledge the Nonwovens Cooperative Research Center at North Carolina State University (NCRC) Project 09-118 for support for W.J.S., and the U.S. Department of Education GAANN Project #P200A100014 for support of B.K.

Notes

The authors declare no competing financial interest.

ACKNOWLEDGMENTS

We thank Christina Devine for helping with SEM imaging performed at Duke University, and Dr. Jess Jur of NC State College of Textiles who helped with the construction of the first version of the ALD reactor. We acknowledge Allasso Industries Inc. for supplying the PA-6 fibers and for SEM images of the untreated fiber cross-sections.

REFERENCES

(1) Fox, R. T.; Wani, V.; Howard, K. E.; Bogle, A.; Kempel, L. *J. Appl. Polym. Sci.* **2008**, *107*, 2558−2566.
(2) Devaux, E.; Koncar, V.; Kim, B.; Campagne, C.; Roux, C.; Rochery, M.; Saihi, D. *Trans. Inst. Meas. Control* **2007**, *29*, 355−376.
(3) Burger, C.; Hsiao, B. S.; Chu, B. *Annu. Rev. Mater. Res.* **2006**, *36*, 333−368.
(4) Jur, J. S.; Sweet, W. J.; Oldham, C. J.; Parsons, G. N. *Adv. Funct. Mater.* **2011**, *21*, 1993.
(5) Wakuda, D.; Suganuma, K. *Appl. Phys. Lett.* **2011**, *98*, 073304.
(6) Varesano, A.; Tonin, C. *Text. Res. J.* **2008**, *78*, 1110−1115.
(7) Xiang, C.; Lu, W.; Zhu, Y.; Sun, Z.; Yan, Z.; Hwang, C.-C.; Tour, J. M. *ACS Appl. Mater. Interfaces* **2012**, *4*, 131−136.
(8) Invernale, M. A.; Ding, Y.; Sotzing, G. A. *ACS Appl. Mater. Interfaces* **2010**, *2*, 296−300.
(9) Li, D.; McCann, J. T.; Xia, Y. *Small* **2004**, *1*, 83−86.
(10) Norris, I. D.; Shaker, M. M.; Ko, F. K.; MacDiarmid, A. G. *Synth. Met.* **2000**, *114*, 109−114.
(11) Chen, D.; Miao, Y.-E.; Liu, T. *ACS Appl. Mater. Interfaces* **2013**, *5*, 1206−1212.
(12) Ding, Y.; Invernale, M. A.; Sotzing, G. A. *ACS Appl. Mater. Interfaces* **2010**, *2*, 1588−1593.
(13) Ge, J. J.; Hou, H.; Li, Q.; Graham, M. J.; Greiner, A.; Reneker, D. H.; Harris, F. W.; Cheng, S. Z. D. *J. Am. Chem. Soc.* **2004**, *126*, 15754−15761.
(14) Little, B. K.; Li, Y.; Cammarata, V.; Broughton, R.; Mills, G. *ACS Appl. Mater. Interfaces* **2011**, *3*, 1965−1973.
(15) Klaus, J. .; Ferro, S. .; George, S. . *Thin Solid Films* **2000**, *360*, 145−153.
(16) Kim, S.-H.; Hwang, E.-S.; Kim, B.-M.; Lee, J.-W.; Sun, H.-J.; Hong, T. E.; Kim, J.-K.; Sohn, H.; Kim, J.; Yoon, T.-S. *Electrochem. Solid-State Lett.* **2005**, *8*, C155−C159.
(17) Kim, S.-H.; Kwak, N.; Kim, J.; Sohn, H. *J. Electrochem. Soc.* **2006**, *153*, G887.
(18) Fabreguette, F. H.; Wind, R. A.; George, S. M. *Appl. Phys. Lett.* **2006**, *88*, 013116.
(19) Fabreguette, F. H.; George, S. M. *Thin Solid Films* **2007**, *515*, 7177−7180.
(20) Wilson, C. A.; Goldstein, D. N.; McCormick, J. A.; Weimer, A. W.; George, S. M. *J. Vac. Sci. Technol., A* **2008**, *26*, 430−437.
(21) Cavanagh, A. S.; Wilson, C. A.; Weimer, A. W.; George, S. M. *Nanotechnology* **2009**, *20*, 255602.
(22) Palmer, R. J. In *Encyclopedia of Polymer Science and Technology*; John Wiley & Sons, Inc., 2002.
(23) Grubbs, R. K.; Nelson, C. E.; Steinmetz, N. J.; George, S. M. *Thin Solid Films* **2004**, *467*, 16−27.
(24) Wilson, C. A.; McCormick, J. A.; Cavanagh, A. S.; Goldstein, D. N.; Weimer, A. W.; George, S. M. *Thin Solid Films* **2008**, *516*, 6175−6185.
(25) Kalanyan, B.; Oldham, C. J.; Losego, M. D.; Parsons, G. N. *Chem. Vap. Deposition* 2013, *19*, in press, 10.1002/cvde.201207053.
(26) Spagnola, J. C.; Gong, B.; Arvidson, S. A.; Jur, J. S.; Khan, S. A.; Parsons, G. N. *J. Mater. Chem.* **2010**, *20*, 4213.
(27) Oldham, C. J.; Gong, B.; Spagnola, J. C.; Jur, J. S.; Senecal, K. J.; Godfrey, T. A.; Parsons, G. N. *J. Electrochem. Soc.* **2011**, *158*, D549−D556.
(28) Jur, J. S.; Spagnola, J. C.; Lee, K.; Gong, B.; Peng, Q.; Parsons, G. N. *Langmuir* **2010**, *26*, 8239−8244.
(29) Elam, J. .; Nelson, C. .; Grubbs, R. .; George, S. . *Surf. Sci.* **2001**, *479*, 121−135.
(30) Sweet, W. J.; Jur, J. S.; Parsons, G. N. *J. Appl. Phys.* **2013**, *113*, 194303.
(31) Chronakis, I. S.; Grapenson, S.; Jakob, A. *Polymer* **2006**, *47*, 1597−1603.
(32) Xia, Y.; Lu, Yun *Compos. Sci. Technol.* **2008**, *68*, 1471−1479.
(33) Miyauchi, M.; Miao, J.; Simmons, T. J.; Lee, J.-W.; Doherty, T. V.; Dordick, J. S.; Linhardt, R. J. *Biomacromolecules* **2010**, *11*, 2440−2445.